Geomechanics and Engineering, *Vol. 15, No. 5 (2018) 1125-1133*
DOI: https://doi.org/10.12989/gae.2018.15.5.1125

Regularity and coupling correlation between acoustic emission and electromagnetic radiation during rock heating process

Biao Kong[1], Enyuan Wang[*2,3] and Zenghua Li[**2,3]

[1]*Key Lab of Mine Disaster Prevention and Control, College of Mining ad Safety Engineering, Shandong University of Science and Technology, Qingdao, Shandong 266590, China*
[2]*Key Laboratory of Coal Methane and Fire Control, Ministry of Education, China University of Mining and Technology, Xuzhou 221116, China*
[3]*School of Safety Engineering, China University of Mining and Technology, Xuzhou, Jiangsu, 221116, China*

(Received May 4, 2017, Revised February 23, 2018, Accepted February 27, 2018)

Abstract. Real-time characterization of the rock thermal deformation and fracture process provides guidance for detecting and evaluating thermal stability of rocks. In this paper, time -frequency characteristics of acoustic emission (AE) and electromagnetic radiation (EMR) signals were studied by conducting experiments during rock continuous heating. The coupling correlation between AE and EMR during rock thermal deformation and failure was analyzed, and the microcosmic mechanism of AE and EMR was theoretically analyzed. During rock continuous heating process, rocks simultaneously produce significant AE and EMR signals. These AE and EMR signals are, however, not completely synchronized, with the AE signals showing obvious fluctuation and the EMR signals increasing gradually. The sliding friction between the cracks is the main mechanism of EMR during the rock thermal deformation and fracture, and the AE is produced while the thermal cracks expanding. Both the EMR and AE monitoring methods can be applied to evaluate the thermal stability of rock in underground mines, although the mechanisms by which these signals generated are different.

Keywords: rock thermal treatment; AE; EMR; coupling correlation

1. Introduction

Deep underground engineering, such as the methods available for radioactive waste disposal, increased exploitation of geothermal resources, and restoration of nearby buildings following a fire accident, is inevitably related to the strength and deformation characteristics of rock structures after high-temperature treatment (Kuenzer and Stracher 2012, Zhou *et al*. 2017, Kong *et al*. 2016a, Cheng *et al*. 2017a, b, Hu *et al*. 2018a, b). Evaluating the mechanical parameters and deformation evolution of rock during the heating process is necessary to analyze the stability of surrounding rock (Kong *et al*. 2016b, Sun *et al*. 2016, Wang *et al*. 2018a, b, c, d).

Many experimental studies and theoretical discussions pertaining to the determination of physical and mechanical parameters of rock after high-temperature treatment; deformation mechanism; rock failure criterion; constitutive relation; and rock thermal cracking mechanism have been conducted (Ozguven and Ozcelik 2014, Zhu *et al*. 2016). Liu and Xu (2000) evaluated the basic mechanical properties of granite under different temperatures (20-600 ℃), and discussed the variation law of elastic modulus, uniaxial compressive strength, with temperature. Guo *et al*. (2015) analyzed the effect of high temperature on the strength and deformation characteristics of marble. Kong *et al*. (2016b) studied the mechanical behavior and fracture evolution of sandstone subjected to high-temperature treatment. Taking sandstone samples as the research material, the influence of temperature on sandstone damage was evaluated by studying the variations in ultrasonic velocity and porosity (Zhao *et al*. 2009).

High-temperature treatment causes thermal damage to the rock, which in turn leads to thermal cracking. During the heat treatment, minerals inside rock masses experience thermal expansion and thermal deformation (Zhao *et al.* 2016, Fan *et al.* 2017, Zhou *et al.* 2018). While most studies focused on the mechanical properties and fracture stability of rock after the temperature treatment, few studies also evaluated the deformation and fracture process of rock materials during the process of continuous heating, real-time reflection, rock thermal deformation and fracture and provided guidance to detect and evaluate the thermal stability of rocks during high-temperature treatment.

AE and EMR are two geophysical phenomena that accompany the deformation and failure of coal and rock materials (Agioutantis *et al.* 2016, Wang *et al.* 2016, Zhou *et al.* 2016, Song *et al.* 2017, Novikov *et al.* 2018). On the basis of a large number of experimental and theoretical studies, the technology of AE and EMR technology has now become an important method to forecast the rock burst, coal and gas outburst (Wang *et al*. 2017, Wen *et al.* 2016a, 2017). Following treatment at different temperatures, AE waves show significant differences in their characteristics during deformation and rupture. The ringing count of the

∗Corresponding author, Professor
E-mail: wey263@yeah.net
∗∗Corresponding author, Professor
E-mail: lzh6512@126.com

ISSN: 2005-307X (Print), 2092-6219 (Online)

AE signal shows a good corresponding relationship with a stress curve, which fully reflects the rupture evolution law of marble in different stages (Guo *et al.* 2015). In the loading process, the frequency and the intensity of AE of the salt rock are increase with the rise of temperature when the temperatures were between 20 and 150℃ (Wu *et al.* 2014).

EMR is closely related to the process of coal rock deformation and fracture (Wang *et al.* 2007, Kong *et al.* 2017a). Many experimental tests were conducted to study the EMR characteristics of coal and rock under loading conditions (He *et al.* 2012, Wang *et al.* 2014). After high-temperature treatment, the process of sandstone deformation and fracture can produce significant EMR signals. The EMR signals increase with an increase in stress (Kong *et al.* 2016a). EMR signals are clearly produced during the coal heating process. During the coal heating process, thermal deformation and thermal cracking occur in the coal body; the free electrons and electric dipoles in the coal body migrate and generate EMR signals. The accumulated EMR pulses and temperature show a linear polynomial development and other changes.

Because of randomness and unexpected and complex reactions that occur during rock thermal deformation and rupture (Xie *et al.* 2015, Wen *et al.* 2016b), a single prediction method often cannot accurately predict rock thermal deformation and rupture. The forecasting and early warning methods should therefore consider the main development direction of rock thermal disasters as well as the rock mechanics and generation of AE and EMR signals. Thus, it is necessary to further study the AE and EMR time-series characteristics as well as the corresponding relationship and internal mechanisms responsible during thermal deformation and fracture of rock.

Accordingly, this paper established the temperature-acoustic-electromagnetic monitoring system during the rock continuous heating process, and synchronously measured the temperature and acoustic-electromagnetic signals during rock thermal treatment. The temperature field variation of rock, the time-series characteristics of acoustic as well as electromagnetic signals, and the coupling correlation of acoustic–electromagnetic signals were analyzed. We also analyzed the principle of acoustic-electromagnetic signals during rock thermal deformation and fracture. By studying the coupling characteristics of AE and EMR under rock continuous heating process, a better understanding of the deformation and failure process of rock as an underground energy storage medium can be obtained. The results have practical value for development of underground engineering resources.

2. Experimental

Large pieces of rock samples (4.6 m in thickness) with good integrity were taken from the immediate roof of 7211 working face in Sanhejian Coal Mine. The samples, which belong to gray fine sandstone and exhibit fine horizontal bedding, are composed of 50.5% of quartz, 15.7% of potassium feldspar, 5.1% of dolomite and 19.1% of clay mineral.

The samples possess blocky, granular and crystalline

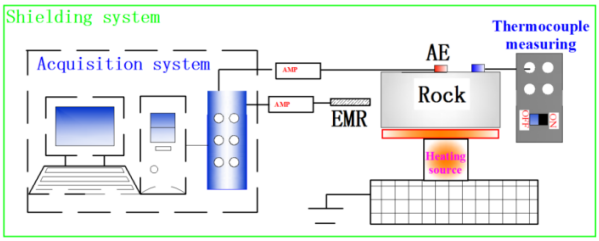

Fig. 1 Experimental system

structures with good homogeneity and an average density of 3.06 g/cm³.After being collected, they were processed in accordance with methods suggested by ISRM–and then made into cylindrical specimens.

The experimental system consists of four parts: the heating device, the temperature measuring device, the EMR and AE signal data acquisition system and the electromagnetic shielding system. The schematic diagram of the experimental setup is depicted in Fig. 1.

A certain distance was kept between the rock sample and the continuous heat source located under the center of the rock sample, so that the rock would be continuously heated from the center to the periphery. A high-precision temperature sensor was used to measure the temperature within the testing range of 0-1300℃ and at a measurement accuracy of 0.5℃. AE and EMR signals were acquired by using the CTA-1 type electro-acoustic dynamic data acquisition system which can simultaneously collect and analyze data of 8 channels. The working mechanism of this system is as follows. First, the signals received by AE and EMR sensors are amplified by the preamplifier and then transmitted into the filter circuit through the coaxial shielded cable. After being filtered, the signals are transmitted into the 16 bits A/D conversion module. Next, the converted digital signal enters the parameter-forming circuit to form AE and EMR parameters which are stored in the buffer and then transmitted to the computer through the PCI bus for further processing and display.

Variations in AE and EMR frequencies aid in the selection of frequency band for fieldwork, and the optimal detection range can be adjusted by choosing the appropriate frequency band. Therefore, the broadband resonant frequency AE sensor R30a (developed by the American Physical Acoustics company) was selected to collect AE signals during the continuous rock heating process. The upper limit of the analyzed frequency range was above 1 MHz. EMR signals were received using a magnetic rod antenna whose frequencies were 1 kHz. In order to reduce the interference of industrial electromagnetic signals, radio broadcasting and communication network to EMR signal reception, all the experiments were carried out in the AFGP-type high-efficiency shielding room. The receiving frequencies of the ferrite rod antenna and the AE sensor are consistent, which can synchronize the collection of AE and EMR signals in the continuous rock heating process.

The experimental procedures are as follows: Before the start of the experiment, the threshold value of the acquisition system was adjusted to make the threshold value of EMR signals higher than that of EMR signals generated by the machine and environment. In this way, the interference of the environment to the experiment could be effectively eliminated. Meanwhile, layouts of the

experimental system and the data acquisition system were adjusted appropriately. The threshold value and sampling rate of the acquisition system were set at 45 dB and 1 MSPS, respectively. The AE preamplifier and EMR preamplifier have a gain of 40 dB and 60 dB, respectively. When the intensity of EMR and AE signals exceeds the threshold value, the high-speed data acquisition system would record the EMR and AE data.

3. Results and discussion

3.1 Characteristics of AE time series signals

AE signals can be received during the rock heating process. The change rules of AE time series signals are shown in Fig. 2.

As can be seen from Fig. 2, the rock can produce clear AE signals under the action of continuous heating source. During the initial period of heating, the rock sample fails to be heated in the beginning, as no clear AE signal is generated during this period. When the rock starts to be heated, the temperature rises rapidly. Accordingly, thermal cracking occurs inside the rock particles, which lead to the breakdown of internal structure of the rock. As the temperature reaches about 70℃, AE signals increase gradually. When the heating time reaches 32 s, the temperature rises rapidly to 135℃. At this moment, the internal parts of rock particles get deformed and ruptured, and great changes take place in the internal structure of rock.

Under the influence of heat accumulation, the rock experiences varied thermal deformation and cracking. At 32 s, the AE energy value has grown to 8770 atto Joule (aJ), and the initial thermal cracking of rock is the most significant in this period. AE energy undergoes fluctuant changes during the continuous heating process. In this period, a certain number of thermal fractures are generated, and the thermal cracking degree is higher than the initial thermal cracking degree. As the temperature exceeds 150 ℃, the energy accumulation and release of internal rock particles decides that the AE energy steps into more obviously a waving and fluctuant state.

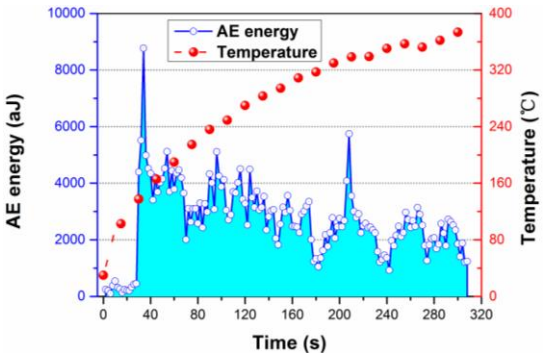

Fig. 2 Characteristics of AE time series

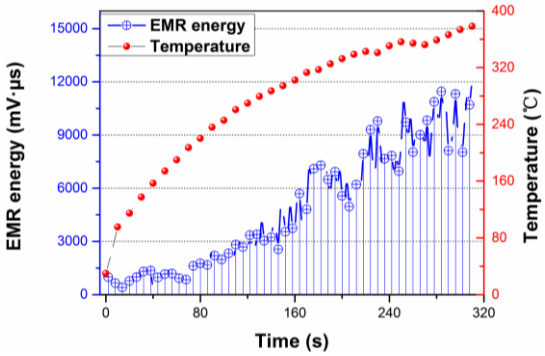

Fig. 3 Characteristics of EMR time series

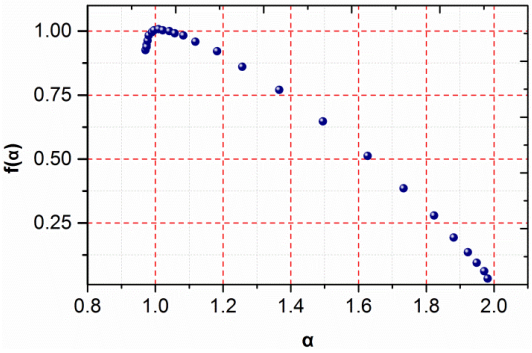

Fig. 4 The multi-fractal characteristic curve

3.2 Characteristics of EMR time series signals

Fig. 3 presents the experimental results when the receiving frequency of EMR antenna is 1 kHz during the heating process.

It can be seen from Fig. 3 that rock can produce clear EMR signals in the continuous heating process. In the initial period of heating, EMR signals are weak, and the EMR energy is small. This is because the temperature has not exceeded the thermal cracking threshold, and the internal part of the sample has changed slightly. With the rise of temperature, EMR signals become more and more variable, and the EMR energy increases gradually.

The EMR time series is nonlinear. The analysis of multi-fractal characteristics of EMR time series can further reveal the relationship between EMR energy and rock thermal deformation rupture status. Based on the multi-fractal calculation process (Kong *et al*. 2016c), the multi-fractal spectrum of EMR signals was calculated, and the changing trends of spectral characteristic parameters were studied. Fig. 4 displays the multi-fractal characteristic curve of EMR signals during rock continuous heating.

According to the multi-fractal theory, the multi-fractal spectral morphology has two forms: The first is “the intensive spectrum” in which the spectral shape deviates to the right side, below the left side, indicating that large signals play an important role in the EMR time series. The second is “the sparse spectrum” where the spectral shape deviates to the left side, below the right side; in this case, small signals play an important role in the EMR time series and the discreteness of the EMR information is obvious.

The discreteness of the EMR information is very clear, as illustrated in Fig. 4. The multi-fractal spectral morphology here belongs to “the sparse spectrum”. Compared with large signals, small signals which play a significant role in EMR time series are more likely to

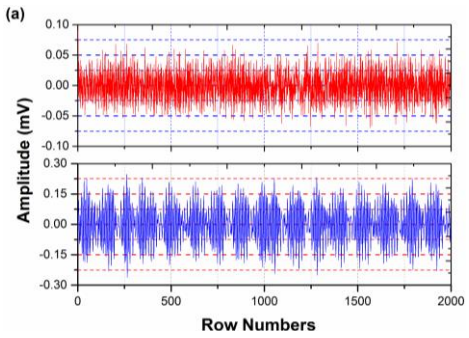

(a) AE waveforms

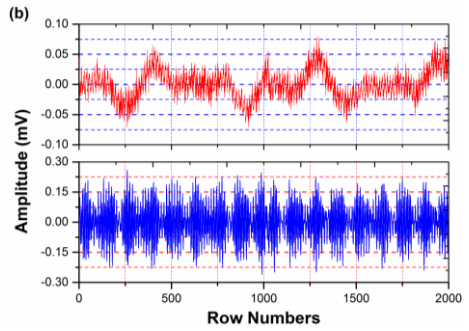

(b) EMR waveforms

Fig. 5 The change characteristics of AE and EMR waveforms in different temperature ranges

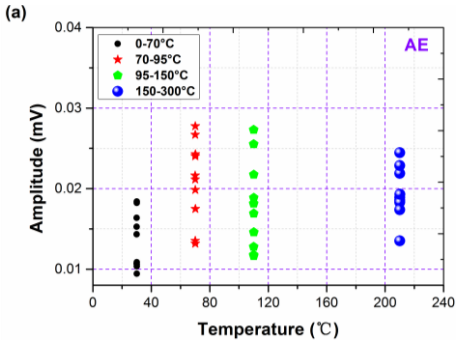

(a) Amplitude of AE signal

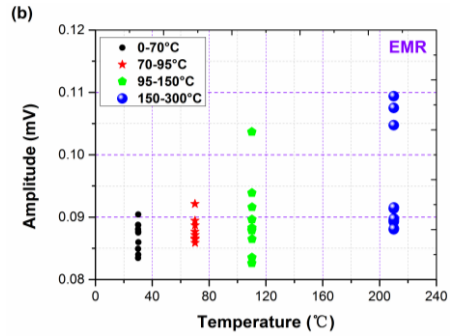

(b) Amplitude of EMR signal

Fig. 7 Amplitude characteristics of AE and EMR signals in different temperature ranges

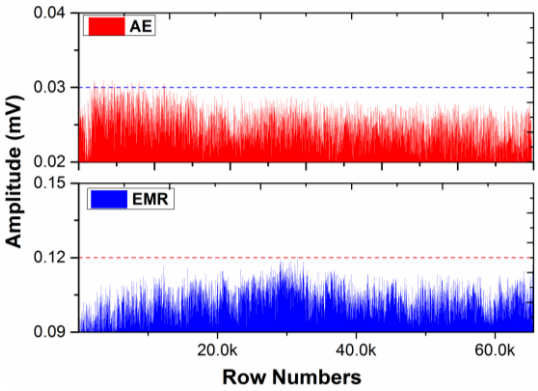

Fig. 6 Amplitude characteristics of AE and EMR signals

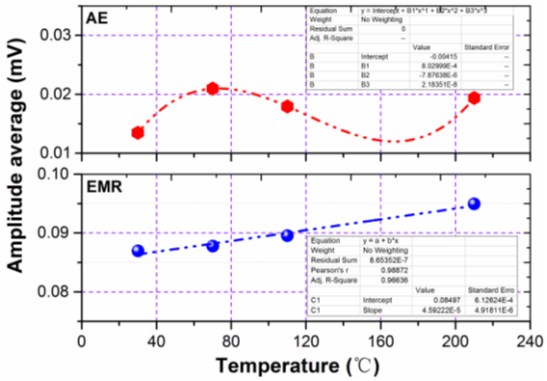

Fig. 8 Changes of average amplitudes of AE and EMR signals

appear. The intensity of EMR signals corresponds to the degree of rock deformation and cracking; large EMR signals indicate that the rock has experienced substantial deformation and rupture. Small signals cover a large proportion of the whole rock deformation and cracking process under continuous heating. The multi-fractal spectrum width Δα reflects the different characteristics of EMR signals. Under the condition of continuous heating, Δα=1.01, which demonstrates the significant changes in both large and small signals. It is well-known that rock deformation and cracking is a complex process (Kong *et al*. 2016c), but its complexity also diminishes in the continuous heating process.

3.3 Coupling correlation of AE and EMR signals

During the continuous heating process, the AE and EMR signals produced due to rock thermal deformation and cracking exhibit regular fluctuations. The variation trends of EMR and AE signals in the heating process are not consistent. AE signals change in multiple phases as they rise first and then drop, while EMR signals which are more active than AE signals increase gradually.

The characteristics of AE and EMR signals in different temperature ranges are analyzed by taking the AE and EMR waveforms in the ranges of 70-95℃ and 150-300 ℃ as an example. The change characteristics of AE and EMR waveforms are shown in Fig. 5.

The variations of EMR and AE signals differ in terms of time series, that is, their local changes are not synchronized. In the temperature range of 70-95℃, the amplitude intensity of EMR signals is obvious greater than that of AR signals. In the temperature range of 150-300℃, the variation in AE waveform is relatively obvious, and the amplitude change is large. EMR signals change more

abundantly with relatively dense signals and more obvious amplitude change. Since changes of AE and EMR signals are not synchronized, it is difficult to achieve one-to-one correspondence.

The amplitude characteristics of AE and EMR signals in the continuous heating process are exhibited in Fig. 6.

As shown in Fig. 6, as the temperature rises, intensities (amplitudes) of AE and EMR signals change correspondingly. The amplitude of AE signals increases first, then decreases slightly and finally increases again gradually. In contrast, the amplitude of EMR signals is low at the early heating stage, but it grows as the temperature rises; during the later heating period, it remains at a high level. The amplitude fluctuations of AE and EMR signals are not synchronized.

The amplitudes of AE and EMR signals in different temperatures ranges are presented in Fig. 7.

In different temperature ranges, the change trend is more obvious than that at the initial stage of the heating. In the temperature range of 70-95 ℃, the amplitude of AE signals increases. The range of 70-95 ℃ sees the highest intensity of AE signals, followed by the ranges of 95-150 ℃ and 150-300 ℃, and the initial temperature range of 0-70 ℃ witnessed the lowest intensity of AE signal, which reflects the thermal cracking process caused by the temperature treatment. The intensity of EMR signals changes remarkably during the later heating stage: Its amplitude increases and reaches the maximum when the highest temperature is reached.

The changes of average amplitudes of AE and EMR signals in different temperature ranges are simulated, as shown in Fig. 8.

As can be observed from Fig. 8, the change of average amplitude of AE signals with temperature exhibits a polynomial development in the heating process. Specifically speaking, an obvious deformation and crack initiation process occurs in the temperature range of 70-95 ℃, where the initiation and development of cracks in the rock lead to significant changes in AE signals. In contrast, the average amplitude of EMR signals changes linearly with temperature, indicating continuous thermal deformation and cracking of the rock. In other words, the higher the temperature, the larger the average amplitude of EMR signals, and thus the more serious the thermal deformation and cracking.

The variation characteristics of AE and EMR amplitudes reflect the thermal deformation and cracking process of rock. Besides, their variations are not completely synchronized due to their different mechanisms.

3.4 AE and EMR coupling generation mechanisms during rock heating

Rock is composed of different heterogeneous mineral, and the expansion coefficients of various rock minerals differ under the high temperature conditions. Therefore, deformation of rock mineral grains after heating is also different (Wang *et al*. 2016). However, in order to maintain the continuity of its deformation, as a continuum, the internal mineral particles of the rock specimen could not be kept the corresponding inherent thermal expansion

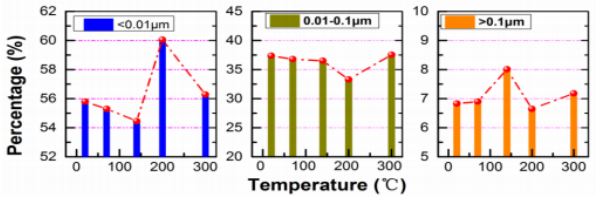

Fig. 9 Changes of percentage of different-sized cracks with the temperature (Rong *et al*. 2015)

coefficient with the temperature. As a result, mineral particles are constrained; larger deformation particles are compressed, while small deformation particles are stretched. The internal rock specimen forms a structural stress which is called the thermal stress (Hang *et al*. 2006). The maximum value of the stress often lies at the junction of mineral particles; if the stress here reaches or exceeds the limit strength of the rock, the bond between the mineral particles along the interface will break, resulting in thermal cracking.

According to the above analysis, the effect of temperature on rock pore structure is as follows: When the temperature of rock rises, the adsorbed water in the rock will evaporate (Sun *et al*. 2016). With the further rise of temperature, the minerals that make up the rock are dehydrated; at this time, chemical changes take place, and the rock porosity increases (Kong *et al*. 2016a). In the process of heating, the rock particles will expand and deform, and thereby produce large thermal stress. The thermal stress will cause the generation of micro-cracks which will further extend or generate new cracks at the particle contact surface with the rise of temperature (Zhang *et al*. 2015). The number of cracks in fine sandstone increases sharply and reaches the peak value at 150 ℃, while the number of macro cracks descends when the temperature exceeds 210 ℃ (Rong *et al*. 2015). The changes of percentage of different-sized cracks with the temperature are shown in Fig. 9, where the abscissa represents the temperature and the ordinate represents the percentage of different-sized cracks in the temperature ranges.

It can be seen from Fig. 9 that the distribution of different-sized cracks changes greatly with the rise of temperature. From 70℃ to -300℃, the porosity and effective porosity increases slightly on the whole with the rise of temperature. However, the trend of change varies in different temperature range. Specifically, the range of 70-110℃ does not see the generation of a lot of new micro-cracks in the rock, so the porosity changes little; however, the effective porosity decreases sharply at 110℃. When the temperature steps into the range of 110-140℃, the effective porosity is reduced. In the range of 140-200℃, the effective porosity rises instead.

3.4.1 AE and EMR generation mechanisms

(1) AE generation mechanism

AE events always occur when a sudden slip takes place over a certain area and thereby frees the stored energy (Zhang *et al*. 2014). AE, which can produce event data to interpret the crack propagation of the material, is used to detect and measure the transient wave generated from the

discrete acoustic waves produced by each micro-crack (Shao *et al*. 2015, Kong *et al*. 2017a). There are distinct AE phenomena in sandstone under the effect of temperature, and 70-90℃ is been found to be the threshold for the development of sandstone cracking (Hang *et al*. 2006).

AE signals have a good correspondence with the rock deformation and cracking process. The change characteristics of AE signals in the process of heating are mainly manifested in four stages (Zhang *et al*. 2006): (1) The enhancement stage: Micro-cracks are generated, expanded and connected during the initial stage of heating; (2) The low level stage: The deformation and failure of rock tend to be stable. (3) The second or multiple enhancement stage: New structures are generated after the transformation of internal minerals takes place. (4) The second or multiple decline stage: The mineral structure undergoes further changes at higher temperatures.

In the process of rock thermal failure, the thermal stress causes the closure of primary fractures, thus producing new cracks; besides, the expansion and connection also takes place between cracks. In the process of rock deformation and cracking, AE signals are also produced in the following situations: (1) Under the effect of thermal stress, failure such as the shearing slip of various minerals and cements shearing will result in the generation of AE signals. (2) In the process of the crack initiation, AE signals can be detected during the generation of new cracks. (3) In the process of crack development, AE signals can also be generated under the interaction between friction and collision. Therefore, the slip and shift may occur between rock internal particles during the heating.

(2) EMR generation mechanism

From the microscopic point of view, in the heating process, micro-cracks in the rock expand under the action of thermal deformation and stress, leading to the separation of electric charge (Wang *et al*. 2014) at the crack tip. In fact, the electric charge is the opposite on both sides of crack tip. With the expansion of a large number of micro-cracks, the electric charges accumulate and form an electric field finally. The electromechanical effects (including the piezoelectric effect and the tribo electrification) and the electro-kinetic effect of the rock may be the sources of EMR signals (He *et al*. 2012).

The rock mass releases energy quickly during its thermal deformation and cracking. As one of the most significant energy forms, EMR signals are attributed to the combined action of transient variation that induces electric dipole, the variable velocity motion of separated charges at the crack tip, as well as the fracture expansion and the relaxation of separated charges on fracture walls in the deformation and cracking process.

In this process, free electrons are produced by friction electrification and crack propagation. The change of EMR signals is related to many factors, such as the elastic modulus, internal defect distribution, material heterogeneity, porosity, water content and other physical properties of the material itself (Wang *et al*. 2007).

In the interior of the rock, the weak van der Waals force mineral particles and other minerals and cements combine with each other. The incomplete disappearance of charges on both sides of the charge-carrying layer during the rapid separation of cracks leads to the separation of charges. At the same time, under the effect of thermal stress, rock particles and other minerals and cements start to undergo slide and shift and produce free charges whose variable speed motion can generate EMR signals.

3.4.2 Difference of AE and EMR generation mechanisms

Experiments of EMR in the deformation and cracking process were performed for studying its regularity and discuss and analyze its mechanism. It is proved that EMR and AE are not strictly synchronous, as EMR signals outnumber AE signals and are more closely related to the deformation and cracking of coal or rock (Wang et al. 2006). Based on the experimental results and the theoretical analysis of microcosmic mechanism of coal cracking (Wang et al. 2007), it is considered that the generation of EMR signals is mainly attributed to the sliding friction between cracks during coal cracking, whereas AE signals are produced during the cracks expanding, which well interprets the characteristics of AE and EMR activities in the cracking process.

Temperature would force the water within rock, a kind of natural inhomogeneous mineral, to volatilize in the whole process of burning and heating, which induces the expansion of rock and the formation of thermal stress. After the phase analysis, the XRD energy spectrum curve of rock is obtained, as shown in Fig. 10.

Under the condition of low temperature, quartz can also subject to crystal transformation, for example, α phosphorus quartz–β quartz (163℃)–γ phosphorus quartz (117℃). At 180°C, α square quartz phase changes into β square quartz. However, despite the rapid conversion at the low temperature, neither the structure nor the volume changes radically. The quartz in coal and rock may react with AL_2O_3 and CaO in the combustion process to form a new mineral amorphous vitreous material (Chen *et al*. 2005). Changes in mineral composition during the heating are listed in Table 1.

Table 1 demonstrates that clay minerals and phyllo-silicates are more sensitive to heat and experienced several transformations at elevated temperatures. The process of rock thermal deformation and cracking leads to rapid outward energy release. With the rise of temperature, the increasing internal thermal stress of the rock causes many cracks to develop, become dense and connect. The micro-cracks gradually expand into large cracks until the whole structure is destroyed. In addition, during the thermal deformation and cracking, EMR signals are produced due to the mutual friction and shift of the rock internal particles. For clay-minerals, desorption reaction releases absorbed water between layers and in structural channels, and the number of cracks inside the rock will increase with the rise of temperature. During the thermal deformation and cracking (including the phase transformation), the generation of EMR signals is mainly attributed to the sliding friction between cracks during the cracking, whereas AE signals are produced in the cracks expanding process.

AE and EMR signals are the most significant energy forms. With the rise of temperature, the increasing internal thermal stress of rock causes lots of cracks to develop, become dense and connect; in this process, micro-cracks

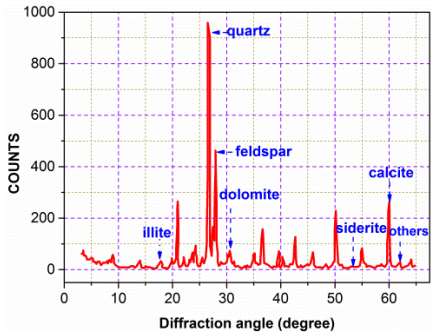

Fig. 10 The XRD energy spectrum curve

Table 1 Changes in mineral composition by heat (Hajpál and Török 2004)

Rock sample	Mineral	Changes in mineral component at ℃			
		22	150	300	450
Balatonrendesi	Kaolinite		+		
	Hematite				+
	Goethite		+		+
Ezu¨sthegyi	Chlorite		+		
	Kaolinite			+	
Rezi	Jarosite		+		
Cottaer	Glauconite			+	
Donzdorfer	Calcite			+	

*Partial data, "+" and shaded area marks the range where mineral is present

gradually expand into large cracks until the whole structure is destroyed. In addition, during the thermal deformation and cracking, AE and EMR signals will be produced due to the mutual friction and shift of the rock internal particles.

EMR and AE signals are not consistent in terms of the overall trend of local changes, so their change characteristics are opposite in different stages, indicating the different generation mechanisms between EMR and AE. Moreover, the correlation in EMR and AE signals is different. Therefore, EMR and AE signals are negatively correlated at the 1% stress levels and have no obvious corresponding relationship at the same time (Kong *et al*. 2016a). The difference in the changes between EMR and AE signals is caused by their different mechanisms for signal generation. Thermal deformation and thermal cracking occur in rock under the action of continuous heat source. AE signals are produced by thermal crack propagation, whereas EMR signals are produced by rock deformation and internal crack sliding friction as the free electrons and electric dipole in rock migrate and generate electromagnetic wave.

The frequency, amplitude, energy, time and the change of AE signals are affected by the intensity, uniformity, grain size, the number of primary fractures and the degree of compaction. The structure of treated materials is actually affected by the temperature-induced processes. At the most elevated temperatures, a substantial number of intra-granular cracks appear. The competition between different crack populations also depends on the physical and mechanical properties of materials (Chmel and Shcherbakov 2014). The frequency-amplitude characteristics of AE signals provide a new means and basis on the damage evolution and mechanism of rock deformation and cracking after the high temperature treatment (Kong *et al*. 2017a).

The EMR frequency is related to the width of rock cracks (Rabinovitch *et al*. 2002). By analyzing the characteristics of EMR frequency spectrum, it is possible to obtain more comprehensive data in the deformation and cracking process under the action of continuous heat source. EMR can reflect the temperature changes as well as deformation and failure process during the heating (Wang *et al*. 2016). Using change characteristics of EMR signals during the heating for reference, a conceptual design of a method of detecting concealed fire in underground mine has been presented (Kong *et al*. 2017b). The EMR count can well reflect the process of rock deformation and cracking after high-temperature treatment.

4. Conclusions

In this paper, the time -frequency characteristics of AE and EMR signals were studied by conducting experiments during the whole process of rock continuous heating. The coupling correlation between AE and EMR signals during rock thermal deformation failure was analyzed.

• During continuous heating, rocks simultaneously produce significant AE and EMR signals. AE signals increases first and then decreases, as the temperature increases, AE signals then showed the increase–decrease cycle process. The increasing trends of EMR signals are from slow growth to rapid growth. AE and EMR signals are not completely synchronized, with AE signals showing obvious fluctuation while the EMR signals increase gradually.

• During different temperatures stages, the AE amplitude increased and the change trend is obvious than the initial stage of the heating. The temperature is range is between in the range of 70-95℃, the AE intensity increases, and the eventually intensity reaches the maximum value. The intensity of AE is the largest, and the strength value is higher than the 95-150℃ and 150-300℃ temperature stage. The intensity of EMR signals changes significantly during the latter heating stage, the amplitude increased and reached the maximum when the temperature increases to the maximum

• For clay-minerals, desorption reaction releases absorbed water between layers and in structural channels, the number of cracks inside the rock will increase with the temperature increase .Under the condition of low temperature, quartz crystal transformation can also occur. During rock thermal deformation and fracture (including the phase transformation), the sliding friction between the cracks is the main mechanism of EMR during the coal fracture, and the AE is produced while the cracks expanding.

• Under different temperature stages, the local variations of AE and EMR signals are different. The difference in the changes between the EMR and AE signals is that the

mechanisms by which these signals are generated are different. Both the EMR and AE signals can be generated from rock materials under the action of continuous heat source. The EMR and AE monitoring methods can thus be applied to evaluate the thermal stability of rock materials in underground engineering.

Acknowledgements

The research described in this paper was financially supported by the Fundamental Research Funds for the Central Universities (2018CXNL02) and A Project Funded by the Priority Academic Program Development of Jiangsu Higher Education Institutions (PAPD). The authors would like to thank the reviewers and editors who presented critical and constructive comments for the improvement of this paper. We also wish to thank K Anand Kumar and SISTRANS Editorial Services for improving the language of this paper.

References

Agioutantis, Z., Kaklis, K., Mavrigiannakis, S., Verigakis, M., Vallianatos, F. and Saltas, V. (2016), "Potential of acoustic emissions from three point bending tests as rock failure precursors", *J. Min. Sci. Technol.*, **26**(1), 155-160.

Chen, L.J., Zhao, H.B., Gu, H.T. and Chen, J.T. (2005), "Study on Microstructure of Coal Roof Sandstone Under High Temperature", *J. Chin. Univ. Min. Technol.*, **34**(4), 443-446.

Cheng, W., Hu, X., Xie, J. and Zhao, Y. (2017a), "An intelligent gel designed to control the spontaneous combustion of coal: Fire prevention and extinguishing properties", *Fuel*, **210**, 826-835.

Cheng, W., Hu, X., Xie, J. and Zhao, Y. (2017b), "Preparation and swelling properties of poly(acrylic acid-co-acrylamide) composite hydrogels", *e-Polymers*, **17**(1), 95-106.

Chmel, A. and Shcherbakov, I. (2015), "Microcracking in impact-damaged granites heated up to 600°C", *J. Geophys. Eng.*, **12**(3), 485-492.

Fan, T., Zhou, G. and Wang, J. (2017), "Preparation and characterization of a wetting agglomeration based hybrid coal dust suppressant", *Proc. Safety Environ. Protect.*, **113**, 282-291.

Guo, Q.L., Rong, G. and Yao, M. (2015), "Experimental study on acoustic emission behaviors and mechanical properties of thermal damaged marbles", *Chin. J. Rock Mech. Eng.*, **34**(2), 3-12.

Hajpál, M. and Török, Á. (2004), "Mineralogical and colour changes of quartz sandstones by heat", *Environ. Geol.*, **46**(3-4), 311-322.

Hang, Y., Qu, F. and Zhao, Y.S. (2006), "Acoustic emission phenomena of thermal cracking of sandstone", *Chin. J. Geotech. Eng.*, **28**(1), 73-75.

He, M.C., Miao, J.L. abd Feng, J.L. (2010), "Rock burst process of limestone and its acoustic emission characteristics under true-triaxial unloading conditions", *J. Rock Mech. Min. Sci.*, **47**(2), 286-298.

He, X.Q., Nie, B.S., Chen, W.X., Wang, E.Y., Dou, L.M., Wang, Y.H., Liu, M.J. and Mitri, H. (2012), "Research progress on electromagnetic radiation in gas-containing coal and rock fracture and its applications", *Saf. Sci.*, **50**(4), 728-735.

Hu, Z.X., Hu, X.M., Cheng, W.M. and Lu, W. (2018), "Influence of synthetic conditions on the performance of melamine-phenol-formaldehyde resin microcapsules", *High Perform. Polym.*, **13**, 1-10.

Hu, Z.X., Hu, X.M., Cheng, W.M., Zhao, Y.Y. and Wu, M.Y. (2018b), "Performance optimization of one-component polyurethane healing agent for self-healing concrete", *Construct. Build. Mater.*, **179**, 151-159.

Kong, B., Wang, E., Li, Z., Wang, X., Chen, L. and Kong, X. (2016c), "Nonlinear characteristics of acoustic emissions during the deformation and fracture of sandstone subjected to thermal treatment", *J. Rock Mech. Min. Sci.*, **90**, 43-52.

Kong, B., Wang, E., Li, Z., Wang, X., Niu, Y. and Kong, X. (2017a), "Acoustic emission signals frequency-amplitude characteristics of sandstone after thermal treated under uniaxial compression", *J. Appl. Geophys.*, **136**, 190-197.

Kong, B., Wang, E.Y., Li, Z.H. and Niu, Y. (2017b), "Time-varying characteristics of electromagnetic radiation during the coal-heating process", *J. Heat Mass Transfer*, **108**, 434-442.

Kong, B., Wang, E.Y., Li, Z.H., Wang, X.R., Liu, J. and Li, N. (2016b), "Fracture mechanical behavior of sandstone subjected to high-temperature treatment and its acoustic emission characteristics under uniaxial compression conditions", *Rock Mech. Rock Eng.*, **49**(12), 4911-4918.

Kong, B., Wang, E.Y., Li, Z.H., Wang, X.R., Liu, X.F., Li, N. and Yang, Y.L. (2016a), "Electromagnetic radiation characteristics and mechanical properties of deformed and fractured sandstone after high temperature treatment", *Eng. Geol.*, **209**, 82-92.

Kuenzer, C. and Stracher, G.B. (2012), "Geomorphology of coal seam fires", *Geomorphology*, **138**(1), 209-222.

Liu, Q.S. and Xu, X.C. (2000), "Damage analysis of brittle rock at high temperature", *Chin. J. Rock Mech. Eng.*, **19**(4), 408-411.

Novikov, E.A., Oshkin, R.O., Shkuratnik, V.L., Epshtein, S.A. and Dobryakova, N.N. (2018), "Application of thermally stimulated acoustic emission method to assess the thermal resistance and related properties of coals", *J. Min. Sci. Technol.*, **28**(2), 243-249.

Ozguven, A. and Ozcelik, Y. (2014), "Effects of high temperature on physico-mechanical properties of Turkish natural building stones", *Eng. Geol.*, **183**, 127-136.

Rabinovitch, A., Bahat, D. and Frid, V. (2002), "Similarity and dissimilarity of electromagnetic radiation from carbonate rocks under compression, drilling and blasting", *J. Rock Mech. Min. Sci.*, **39**(1), 125-129.

Rong, H.R., Bai, H.B. and Wang, Z.S. (2015), "Experimental research on mechanical properties and microstructure change law of red sandstone after different temperatures", *Rock Soil Mech.*, **36**(2), 463-469.

Song, D.Z., Wang, E.Y. and Li, Z.H. (2017), "EMR: An effective method for monitoring and warning of rock burst hazard", *Geomech. Eng.*, **12**(1), 53-69.

Sun, Q., Lu, C., Cao, L.W. and Li, W.C. (2016), "Thermal properties of sandstone after treatment at high temperature", *J. Rock Mech. Min. Sci.*, **85**, 60-66.

Wang, E.Y., Jia, H.L., Song, D.Z., Li, N. and Qian, W.H. (2014), "Use of ultra-low-frequency electromagnetic emission to monitor stress and failure in coal mines", *J. Rock Mech. Min. Sci.*, **70**, 16-25.

Wang, E.Y., Kong, B., Liang, J.Y., Liu, X.F. and Liu, Z.T. (2016), "Experimental study of electromagnetic radiation during coal heating", *J. China Univ. Min. Technol.*, **45**(2), 205-210.

Wang, H., Nie, W., Cheng, W., Liu, Q. and Jin, H. (2018a), "Effects of air volume ratio parameters on air curtain dust suppression in a rock tunnel's fully-mechanized working face", *Adv. Powder Technol.*, **29**(2), 230-244.

Wang, H., Cheng, W., Sun, B., Yu, H. and Jin, H. (2018b), "The impacts of the axial-to-radial airflow quantity ratio and suction distance on air-curtain dust control in a fully mechanized coal face", *Environ. Sci. Pollut. Res.*, **25**(8), 7808-7822.

Wang, C., Xiao, Y., Li, Q., Deng, J. and Wang, K. (2018c), "Free

radicals, apparent activation energy, and functional groups during low-temperature oxidation of jurassic coal in northern Shaanxi", *J. Min. Sci. Technol.*, **28**(3), 469-475.
Wang, J., Kang, H., Liu, J., Chen, P., Fan, Z. and Yuan, W. (2018d), "Layout strategic research of green coal resource development in china", *J. China Univ. Min. Technol.*, **47**(1), 15-20.
Wang, X., Wen, Z., Jiang, Y. and Huang, H. (2017), "Experimental study on mechanical and acoustic emission characteristics of rock-like material under non-uniformly distributed loads", *Rock Mech. Rock Eng.*, **51**(3), 729-745.
Wang, Y.H., He, X.Q. and Dou, L.M. (2007), "Study on regularity and mechanism of acoustic emission and electromagnetic emission during fracture process of coal samples", *Chin. J. Geophys.*, **50**(5), 1569-1575.
Wen, Z., Wang, X., Chen, L., Lin, G. and Zhang, H. (2017), "Size effect on acoustic emission characteristics of coal-rock damage evolution", *Adv. Mater. Sci. Eng.*, **2**, 1-8.
Wen, Z.J, Tan, Y.L, Han, Z.Z. and Meng, F.B. (2016a), "Construction of time-space structure model of deep stope and stability analysis", *Polish J. Environ. Stud.*, **25**(6), 2633-2639.
Wen, Z., Wang, X., Tan, Y., Zhang, H., Huang, W. and Li, Q. (2016b), "A study of rock burst hazard evaluation method in coal mine", *Shock Vib.*, (16), 1-9.
Wu, G., Zhai, S.T. and Sun, H. (2014), "Experimental study of acoustic emission of sale rock under high temperature", *Chin. J. Rock Mech. Eng.*, **33**(6), 1203-1211.
Xie, H.P., Gao, F. and Ju, Y. (2015), "Research and development of rock mechanics in deep ground engineering", *Chin. J. Rock Mech. Eng.*, **34**(11), 2161-2178.
Zhang, Y., Liang, P., Liu, X., Liu, S. and Tian, B. (2015), "Experimental study on precursor of rock burst based on acoustic emission signal dominant-frequency and entropy", *Chin. J. Rock Mech. Eng.*, **34**(S1), 2959-2967.
Zhang, Y., Qu, F. and Zhao, Y.S. (2006), "Acoustic emission phenomena of thermal cracking of sandstone", *Chin. J. Geotech. Eng.*, **28**(1), 73-75.
Zhang, Z.Z. and Gao, F. (2015), "Experimental investigations on energy evolution characteristics of coal, sandstone and granite during loading process", *J. Chin. Univ. Min. Technol.*, **44**(3), 416-422.
Zhao, H.B., Yin, Z.G. and Chen, L.J. (2009), "Experimental study on effect of temperature on sandstone damage", *Chin. J. Rock Mech. Eng.*, **28**(1), 2783-2789.
Zhou, F., Sun, Y., Li, H. and Yu, G. (2016), "Research on the theoretical model and engineering technology of the coal seam gas drainage hole sealing", *J. Chin. Univ. Min. Technol.*, **45**(3), 433-439.
Zhou, G., Ma, Y., Fan, T. and Wang, G. (2018), "Preparation and characteristics of a multifunctional dust suppressant with agglomeration and wettability performance used in coal mine", *Chem. Eng. Res. Des.*, **132**, 729-742.
Zhou, G., Zhang, Q., Bai, R., Fan, T. and Wang, G. (2017), "The diffusion behavior law of respirable dust at fully mechanized caving face in coal mine: CFD numerical simulation and engineering application", *Process Safety Environ. Protect.*, **106**, 117-128.
Zhu, T.T., Jing, H.W., Su, H.J., Yin, Q., Du, M.R. and Han, G.S. (2016), "Physical and mechanical properties of sandstone containing a single fissure after exposure to high temperatures", *J. Min. Sci. Technol.*, **26**(2), 319-325.